J1.7

ANALYSIS OF RAPID SCAN SATELLITE IMAGERY TO DIAGNOSE TORNADIC
STORMS AND THE ENVIRONMENT IN WHICH THEY FORM

James F.W. Purdom and John F. Weaver

Regional and Mesoscale Meteorology Branch
NOAA/NESDIS
and
Cooperative Institute for Research in the Atmosphere
Colorado State University
Fort Collins, Colorado

1. INTRODUCTION

Geostationary satellite data provides valuable mesoscale to storm scale information concerning characteristics of severe and tornadic storms and the mesoscale environment in which they form. In the sections that follow, selected aspects of the severe and tornadic storm's mesoscale environment as observed using satellite data are discussed. Parts of those sections deal with the types of analyses that could be undertaken at a local NWS office using advanced satellite data sources, such as rapid scan GOES imagery, along with interactive analysis techniques that should be available through National Weather Service Modernization. Emphasis is on a recent tornado outbreak where rapid scan imagery was available: April 26, 1991. That study does not go into a detailed inspection of conventional data sources, but rather examines the type information available from analysis of GOES-7 imagery that was taken during that outbreak.

2. SATELLITE DATA

During outbreaks of severe weather, the GOES satellite is often placed in a rapid interval imaging mode, termed RISOP, to support operations at the National Severe Storm Forecast Center. When in the RISOP mode, GOES-7 images the continental USA every 15 minutes beginning one minute after the hour, with the following exceptions (all times GMT): 0001 - 0031; 0401 - 0431; 0931 - 1101; 1601 - 1631; and 2131 - 2201. RISOP also includes rapid interval imaging with four 5 minute interval images taken beginning 11 minutes after the hour and half hour from 1231 - 1501 GMT, 1831 - 2100 GMT, 0031 - 0300 GMT and 0631 - 0900 GMT.

Certain principles must be kept in mind when inspecting the GOES imagery that follows. First, since GOES imagery depicts clouds over a curved earth, a parallax adjustment must be made to place a storm's top over its actual ground location. For example, a 60,000 foot storm top near Wichita, Kansas, should be moved just over 19 km back toward the GOES-7 subpoint (at this time 108 deg West). Second, in the

figure captions, times are for the beginning of the satellite's scan sequence: GOES-7 takes just under three and one half minutes to scan southward to the Kansas/Oklahoma boarder. Therefore, a scan sequence beginning at 17:46:00 GMT reaches the Kansas and Oklahoma boarder at 17:50:22 GMT. Finally, a satellite image, or a series of images, represent on-going dynamic and thermodynamic processes in the atmosphere: what is important is to recognize those processes.

3. THE APRIL 26, 1991 TORNADO OUTBREAK

During the afternoon and evening of April 26, 1991, a line of severe thunderstorms developed and moved across Kansas and Oklahoma producing several devastating long track tornadoes, Figure 1.
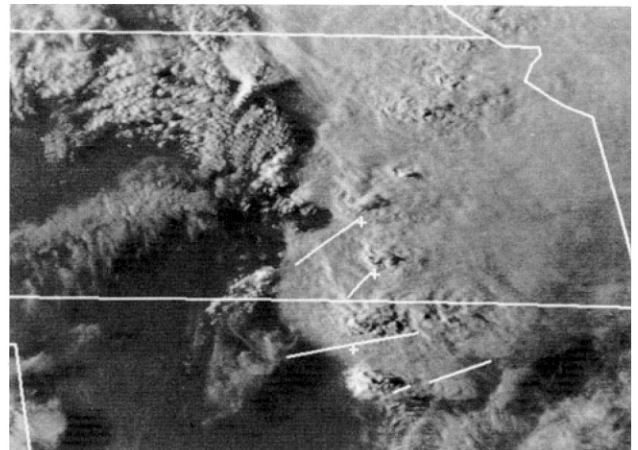

Figure 1. GOES-7 1 km resolution visible image taken at 6:05 PM, CST, on April 26, 1991. Ground tracks of major tornadoes have been added, with a + mark showing the approximate ground location of the tornado at the time of the image. Note that tornado activity has not yet begun with the southern most track.

Analysis of conventional meteorological data at 1200 GMT on the day of the outbreak indicated that Oklahoma and Kansas would be under the threat of strong severe thunderstorms later in the afternoon. At

1200 GMT, NMC upper analyses showed a negatively tilted trough over the Rocky Mountains, with upper level diffluence over the outbreak region. Subsequent GOES-7 cirrus motions clearly show this trough and diffluent flow field, Figure 2. Animation showed the stronger winds associated with the jet stream were moving from eastern New Mexico toward the region of the developing squall line. These strong winds reached the outbreak area a few hours later, Figure 3. When animated in a cloud relative mode (Lubich and Purdom, 1992) satellite imagery showed the above features quite clearly. However, since methods do not exist to show animated sequences in publication, cloud tracking and wind barbs were utilized to illustrate these points in Figures 2 and 3.
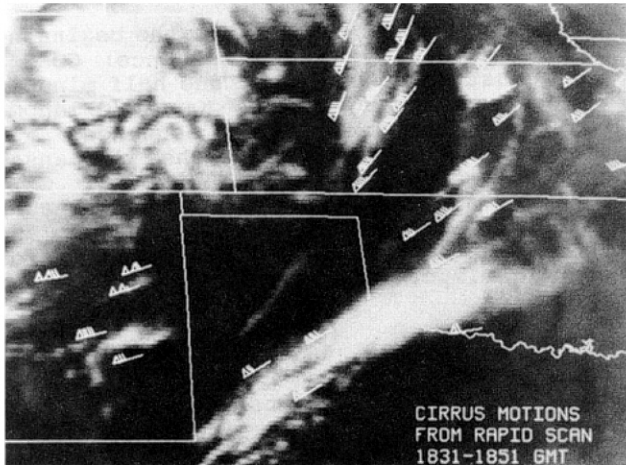

Figure 2. GOES-7 infrared image taken at 1846 GMT on 26 April, 1991. Wind barbs give the direction and speed of cirrus tracers, with speed in knots. Note the maxima in eastern New Mexico.
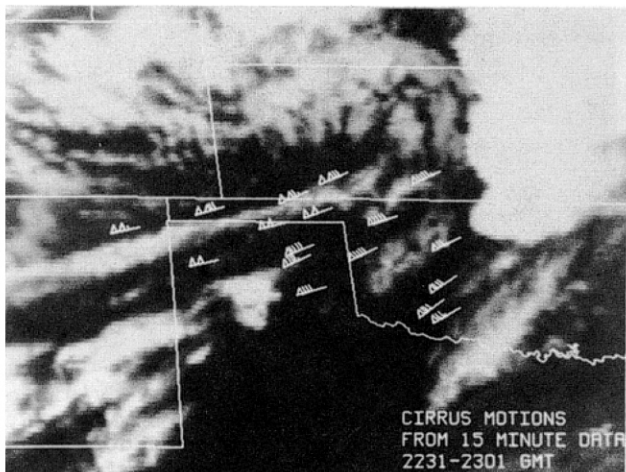

Figure 3. GOES-7 infrared image taken at 2301 GMT on 26 April, 1991. Wind barbs give the direction and speed of cirrus tracers, with speed in knots. The maxima in New Mexico in Figure 2 has moved into the outbreak area. The NMC 300 mb analysis for 00 GMT on the 27th (one hour after this image) showed a wind maxima of 115 kts centered over Dodge City, Kansas.

The NMC 1200 GMT surface analysis showed a region of low pressure in southwestern Nebraska. From that low a Pacific front trailed to the southwest while a dryline extended to the south. A warm frontal boundary was evident across portions of eastern Kansas and Arkansas. During the day those large scale surface features could be followed by combining surface data with the cloud fields evident in satellite imagery, as in Figure 4.

3.1 Pre-storm mesoscale environment

During the early morning of the 26th, severe thunderstorms moved across Oklahoma and southeastern Kansas. At 1235 GMT radar indicated a severe thunderstorm with hail on the Oklahoma and Kansas border. That storm was part of a large mesosystem that was moving out of southeast Kansas into Missouri by 1746 GMT, Figure 4. Rain from that system helped stabilize and moisten air to the north and east of the warm frontal boundary. In NMC analyses after 1500 GMT, that boundary becomes difficult to detect. However, when surface observations are combined with satellite imagery, the boundary is detectable by noting the cooler surface temperatures and dew points and the stable low level clouds to its northeast, Figure 4.
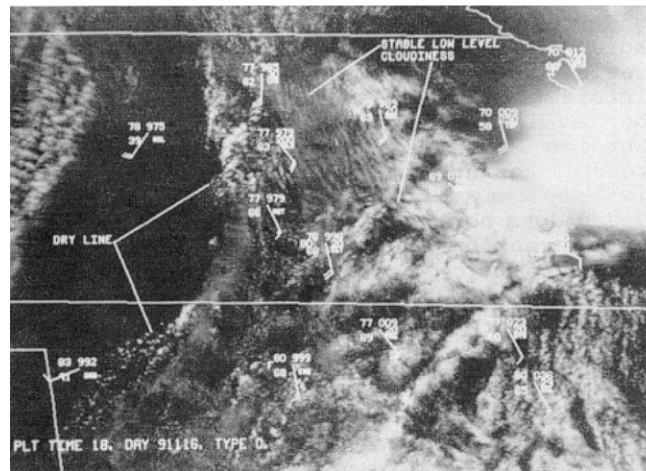

Figure 4. GOES-7 1 km visible image at 1746 GMT with 1800 GMT surface observations. Most surface observations are taken about 10 minutes before the hour and coded for transmission on the hour, while the GOES-7 scan is across the area at almost exactly the same time: thus a 1746 GMT GOES image matches almost exactly in time surface observations for 1800 GMT. Note the cumulus free air and low dew points that existed to the west of the dry line at this time.

The dry line was detectable during the afternoon by combining surface data with GOES-7 visible and infrared imagery. Visible data from GOES-7 shows a distinct difference between the dry, less cloudy air, to the west of the dryline and the moist unstable air to its east, Figure 4. As is typical with afternoon infrared imagery (Purdom, 1991), GOES-7 revealed hotter ground on the dry air side (west) of the dry line versus its moist side (east) where

cooler surface temperatures, a cool moist boundary layer and cumulus cloud contamination combine to result in colder scene temperatures.

3.2 Storm scale environment

In Figure 4, strong cumulus development is evident between Salina (SLN) and Hutchinson (HUT), Kansas, where the dry line and reinforced boundary intersect. An area of strong thunderstorms developed at that intersection and moved north, Figure 5, producing wind damage and weak tornado activity in Nebraska later in the day. At the same time, Figure 5, new storms and growing convective towers are developing along the dry line to the west and southwest of Wichita (ICT). Based on measurements from rapid scan imagery, storm motion at 1846 was from 215 degrees at 35 knots. When that vector was removed from the rapid scan sequence and animation was performed in a storm relative mode, the cumulus to cirrus level shear was found to be greater to the south, Figure 6.
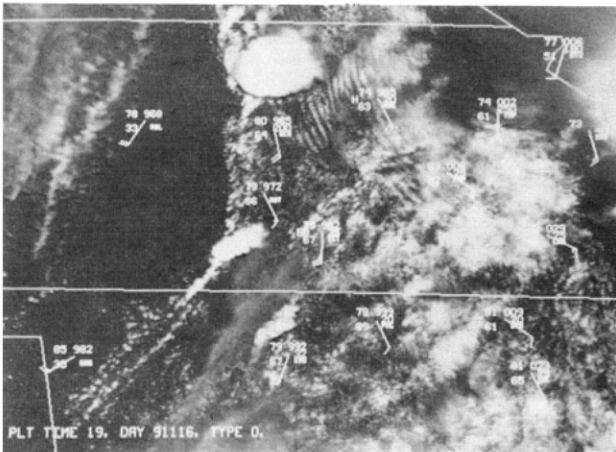
By 1946 GMT, Figure 7, the region of thunderstorm development previously to the west of Wichita had moved north and was producing showers and thunderstorm activity in the Hutchinson area. Immediately southwest of those storms a field of high based cumulus developed in the dry air to the west of the dry line. That organized region of cumulus reflects the movement of strong upper level forcing into that region. All of the major tornadic storms on this day formed south of the point where the northern edge of that cumulus field intersected the dry line. Other indicators of strong vertical forcing moving across the area were an approaching wind maxima, as shown in Figure 3, and an area of cyclonic rotation at mid-levels that was detectable when imagery was animated in a cloud system relative mode.

With movement of stronger winds into the region, the mean movement of the developing storms around the Kansas and Oklahoma border changed from 215 degrees at 35 knots to 235 degrees at 35 knots. In comparing Figure 6 with Figure 8, the

Figure 5. GOES-7 1 km visible image at 1846 GMT with 1900 GMT surface observations.

Figure 7. GOES-7 1 km visible image at 1946 GMT with 2000 GMT surface observations. Note the region of cumulus behind the dry line where dew points are in the high 20s.
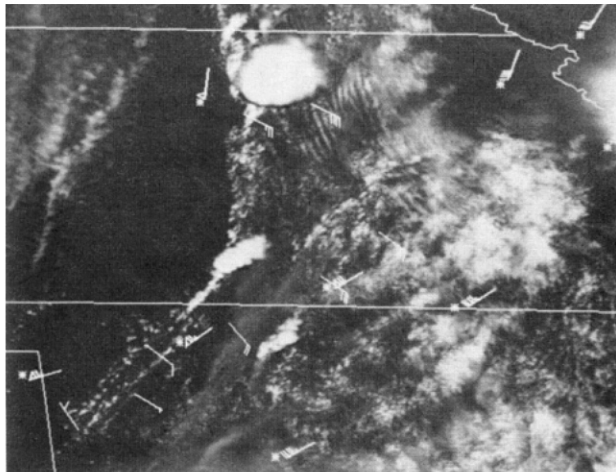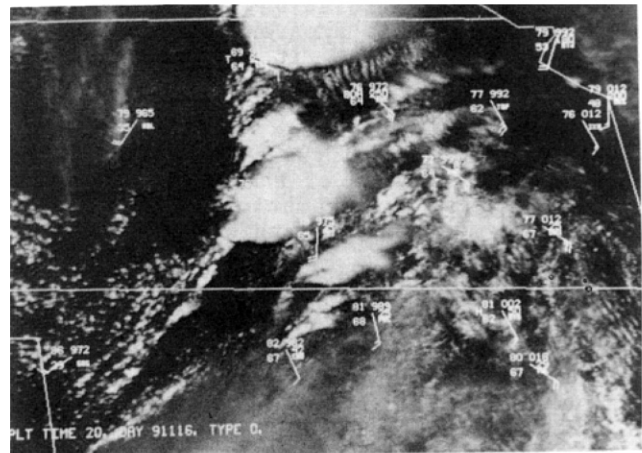

Figure 6. GOES-7 1 km visible image at 1846 GMT with cumulus and cirrus storm relative winds calculated from rapid scan imagery. The relative vector removed is 215 degrees at 35 knots. Cirrus level vectors are denoted by an * at their tail.
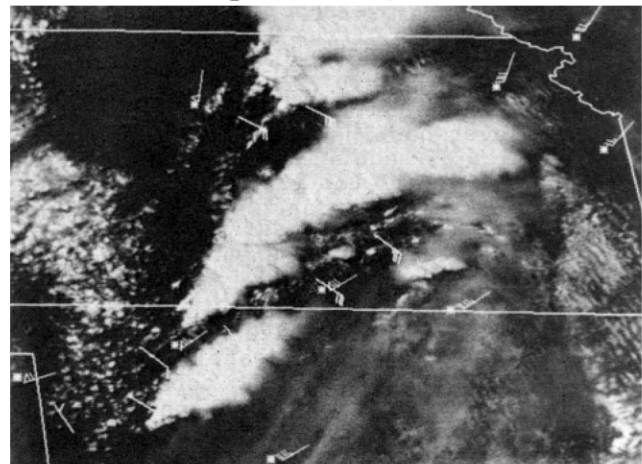

Figure 8. GOES-7 1 km visible image at 2046 GMT with cumulus and cirrus storm relative winds calculated from rapid scan imagery. The relative vector removed is 235 degrees at 35 knots. Cirrus level vectors are denoted by an * at their tail.

cumulus to cirrus relative shear as determined using rapid scan imagery is seen to have increased relative to the southern storms.

Strong veering of storm relative flow between the cumulus and cirrus levels has been noted with other intense tornadic storms (Purdom, 1991).

Among the most important features observed with satellite imagery for this case was the interaction of the storm with its surrounding environment. By 2146 GMT, a fully developed squall line extended across much of Kansas and northern Oklahoma. As shown in Figure 9, immediately to the rear of the storms are low level outflow boundaries. These boundaries are due to rain cooled air left behind by the storms, and reflect the storms' modification of the boundary layer in that region. The importance of that modification for a supercell's evolution to the tornadic phase has been previously discussed by Purdom (1991).

There is strong evidence that the storms blocked the flow at upper levels. When cirrus relative animation was performed, it was apparent that the cirrus slowed down as it approached the thunderstorms, with some of the thinner cirrus dissipating completely. When a vector of 234 degrees at 85 knots was removed from the cirrus motions, the effect of this "blocking" of the upper level flow by the storms was dramatic, Figure 10. One possible mechanism for this deceleration is the development of an upper level region of high pressure associated with the anvil outflow. This upper-level high, coupled with the stabilized boundary layer and region of high pressure associated with the surface outflow mentioned in the previous paragraph, should aid in the development of a rear, mid-level inflow jet, a critical component in a supercell thunderstorm's becoming tornadic.

3.3 Cloud top characteristics

Strong overshooting tops with downstream wake cirrus were produced by the supercells. Those tops were easily detected in visible imagery late in the day, see Figures 1 and 11. As might be expected, those overshooting tops (which are a reflection of each storm's intense updraft) moved parallel to the tornado tracks. Doppler radar at Norman, OK, detected a well defined cyclonic circulation with the storms in Oklahoma. The northern Oklahoma storm was over 130 km from the radar: this indicates that storm was in rotation to great depths. There have been cases where rapid scan visible satellite imagery indicated the overshooting tops of a super cell were in cyclonic rotation (Anderson, 1982). Purdom (1991) found evidence of cyclonic rotation at cloud top when viewing storm relative rapid scan satellite imagery for the Plainfield, Illinois tornadoes of 28 August 1990: that movie sequence was shown during the poster session of this conference (Lubich and Purdom, 1992).
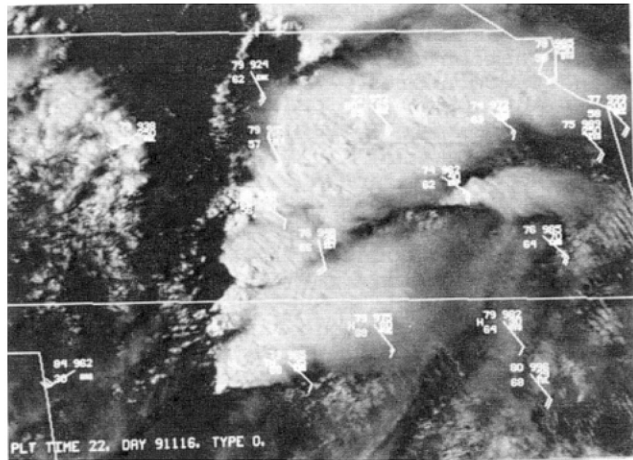

Figure 9. GOES-7 1 km visible image at 2146 GMT with 2200 GMT surface observations. Note the arcs of cumulus behind the storms.
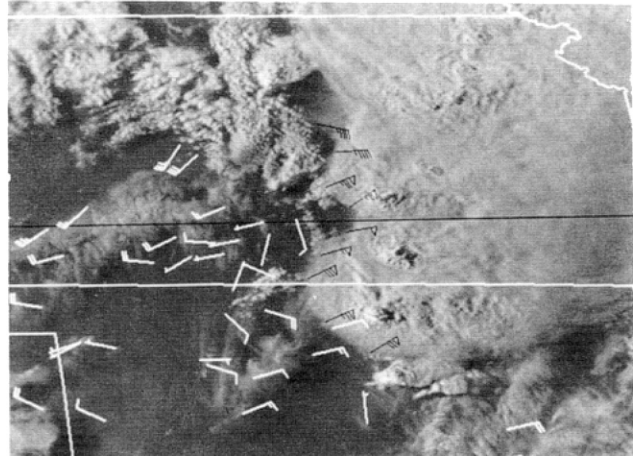

Figure 10. GOES-7 1 km visible image at 2346 GMT with cirrus relative winds calculated from 15 minute interval imagery. The relative vector removed was 234 degrees at 85 knots. In a relative framework, the anvil spread rapidly westward, while cirrus west of the storms reversed its direction of flow as it approached the storms.
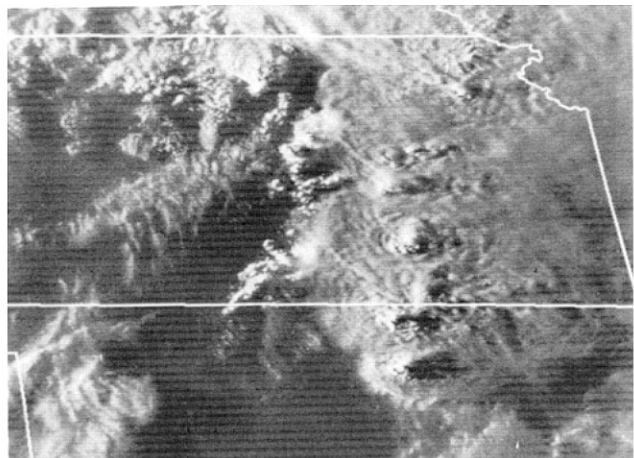

Figure 11. GOES-7 1 km visible image at 0031 GMT, 27 April 1991 showing cirrus plumes at anvil top level streaming downwind from each overshooting top.

Unfortunately, during the April 26, 1991 outbreak no five minute interval imaging was scheduled between 2101 and 0031 GMT: during those times most of the major tornado activity was occurring. This made it impossible to assess whether or not rotation was present at cloud top.

Figure 12 is an enhanced infrared image taken when three of the strongest tornadoes were in progress. In Figure 1, the visible image corresponding to Figure 12, overshooting top regions associated with the tornadic storms are just north of the tornado locations (+).
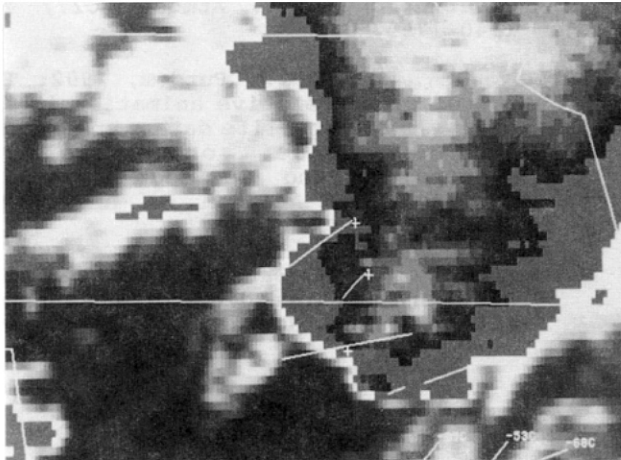

Figure 12. GOES-7, enhanced infrared image at 0001 GMT, 27 April 1991. The bar at bottom of image gives the gray shade associated with -29 C and -53 C. Shading is in increments of 2 C. Tracks of major tornadoes are shown, with (+) marks indicating the approximate ground location of each tornado at the time of the image.

At those same locations in Figure 12, there are no discernable cold overshooting tops. In fact, during the outbreak "classical" infrared severe storm top signatures as described by Heymsfield et al (1983), colder tops with downstream warm wakes, were not observed with the tornadic storms. This was most likely due to the structure of the tropopause in the storm area. Analysis of that rawinsonde data gave an equilibrium level near 200 mb with a corresponding temperature between -53 and -55 C. However, nearby rawinsonde data showed that the lapse rate decreases above the equilibrium level resulting in a temperature of -62 C near 130 mb. This means that wake cirrus in the stratosphere above the anvils had to have been colder, not warmer, than the mean anvil temperature. This appears to be the case when a detailed comparison is made between Figures 1 and 12. Furthermore, in animated visible imagery, thin cirrus from one storm was observed to move across the top of another. Such masking of the anvil could further confuse the analysis of infrared cloud top imagery.

4.   CONCLUSIONS

GOES-7 imagery provided a clear picture of the evolving pre-storm environment. The evolution of important features, including a major trough to the west of the outbreak, diffluent flow over the region and strong winds associated with the jet stream maxima could be monitored using cirrus cloud motions. When imagery was animated in a cloud system relative mode, an area of cyclonic rotation at mid-levels that was detectable and the jet maxima was easily followed as it moved from eastern New Mexico into the region of the developing squall line.

The major focusing mechanism for the outbreak, the dry line, could be followed throughout the day by combining surface data with the cloud fields evident in satellite imagery. Early morning rain from a large mesosystem helped stabilize and moisten air to the north and east of the warm frontal boundary in Kansas. Later in the day, when surface observations are combined with satellite imagery, that boundary is detectable. The first afternoon thunderstorm activity formed where the dry line and reinforced boundary intersected. By 1946 GMT a field of high based cumulus developed in the dry air to the west of the dry line. That organized region of cumulus reflected the movement of strong upper level forcing into the area: all of the major tornadic storms on this day formed south of the point where the northern edge of that cumulus field intersected the dry line.

Rapid scan imagery proved very useful for observing the storms' development and their interaction with the surrounding environment. Since storm development and evolution could be followed so well with that imagery, their direction of movement and its change with time could followed. For example, with movement of stronger upper level winds into the region, the mean movement of the developing storms around the Kansas and Oklahoma border changed from 215 degrees at 35 knots to 235 degrees at 35 knots. Based on those measurements, that vector was be removed from the animation sequence and the cumulus to cirrus level shear was assessed. Strong veering of storm relative flow between the cumulus and cirrus levels was associated with the intense tornadic storms. There is strong evidence that the storms modified their local environment by leaving behind rain cooled air at the surface and blocking the flow at upper levels. This upper level blocking, coupled with the low level modifications to their rear, should aid in the supercell thunderstorms' becoming tornadic.

While certain cloud top signatures associated with severe storms could be detected in visible imagery, this was not the case with infrared imagery. For example, while strong overshooting tops with wake cirrus downstream from these tops were associated with the supercells were detectable in the visible imagery late in the day, there was no corresponding infrared signature. Furthermore, the lack of rapid scan imagery during the time of the major tornado activity made it impossible to determine if cyclonic rotation was evident at cloud top. Forecasters should know under what type circumstances certain signatures, such as infrared cold tops and down stream

warming, should be expected. Investigations should be undertaken to define such regimes.

Storm relative animation is an extremely useful tool for analyzing animated satellite imagery. It should be included as a capability of the advanced interactive systems that will be a part of National Weather Service (NWS) Modernization. That same capability should be made available NOAA's National Centers and incorporated into micro-SWIS if feasible.

Selected parts of the analysis were undertaken using advanced data sources (rapid scan GOES imagery) and a powerful interactive system (a VDUC Wide Word Workstation). Along with other advanced data sources, such data and analysis capabilities will be available as a part of NWS Modernization. Development efforts for advanced meteorological products and analysis techniques must continue with the goal of maximizing the capabilities of those advanced data sets.

Finally, it must be pointed out that a satellite image, or animated sequence of images, represents ongoing dynamic and thermodynamic processes in the atmosphere. The data is best used in conjunction with other meteorological data to understand the unfolding meteorological situation. If satellite data is used in that manner, rather than as a source of "indices" or "signatures," it becomes one of the most valuable meteorological tools available to the forecaster in the stress-filled hours of severe weather occurrence.

5. ACKNOWLEDGEMENTS

6. REFERENCES

Anderson,C.E., 1982: Dramatic development of thunderstorm circulation associated with the Wichita Falls tornado as revealed by satellite imagery. Proc. of the 12th Conf. on Severe Local Storms, San Antonio, TX, Amer. Meteor. Soc., Boston, MA, 493-498.

Heymsfield, G.M., R. Blackmer, Jr. and S. Scholtz, 1983: Upper-Level Structure of Oklahoma Tornadic Storms on 2 May 1979. I: Radar and Satellite Observations. J. Atmos. Sci., 40, 1740-1755.

Lubich, D.A. and J.F.W. Purdom, 1992: The use of cloud relative animation in the analysis of satellite data. Preprints, 6th Conference on Satellite Meteorology and Oceanography, 5-10 January, 1992, Atlanta, GA, Amer. Met. Soc.

Purdom, J.F.W., 1991: Satellite Observations of Severe and Tornadic Storms. Tornado III Symposium, Norman, Ok. In review.